Biochemical and Biophysical Research Communications **282,** 96–102 (2001)
doi:10.1006/bbrc.2001.4558, available online at http://www.idealibrary.com on IDEAL®

Molecular Cloning and Expression of the Novel Splice Variants of K^+ Channel-Interacting Protein 2

Susumu Ohya,* Yuichi Morohashi,† Katsuhiko Muraki,* Taisuke Tomita,† Minoru Watanabe,* Takeshi Iwatsubo,† and Yuji Imaizumi*,[1]

**Department of Molecular and Cellular Pharmacology, Faculty of Pharmaceutical Sciences, Nagoya City University, 3-1 Tanabedori, Mizuhoku, Nagoya 467-8603, Japan; and †Department of Neuropathology and Neuroscience, Graduate School of Pharmaceutical Sciences, University of Tokyo, 7-3-1 Hongo, Bunkyo-ku, Tokyo 113-0033, Japan*

Received January 28, 2001

Two cDNAs encoding the splice variants of K^+ channel-interacting protein 2 (KChIP2) recently reported as human KChIP2 have been identified from rat, mouse, and human heart by RT-PCR. A longer variant, KChIP2L encodes a protein of 270 amino acids, which has a 50-amino-acid insertion in N-terminus in comparison with a shorter one, KChIP2S. Interestingly, both KChIP2S and KChIP2L (KChIP2S/L) but not the original KChIP2 were expressed in human heart and umbilical vein endothelial cells (HUVECs). KChIP2S transcripts but not KChIP2L were predominantly expressed in rat, mouse, and human heart and HUVECs, whereas both transcripts were expressed at low levels in other tissues such as brain, aorta, and kidney. Using chimeric proteins of green fluorescence protein (GFP) fused to the N-terminus of KChIP2S/L, the interactions between Kv4.3 and KChIP2S/L were analyzed in native and Kv4.3-expressed HEK293 cells. Specific localization of GFP-fused KChIP2S/L proteins on or near cell membrane was observed only in Kv4.3-expressed HEK293 cells.

Key Words: **KChIP; A-type K^+ channel; RT-PCR cloning; splice variant; heart; HUVEC; GFP fusion; immunoprecipitation; Kv4.3**

Rapidly inactivating (A-type) K^+ channel currents (I_A) have pivotal roles in the control of action potential threshold, frequency, and duration in excitable cells such as neurons and cardiac and smooth muscle myocytes (1, 2). Among four voltage-dependent K^+ channel subfamilies (Kv1–Kv4), Kv4 subfamily is the leading candidate of K^+ channel genes encoding I_A in several cell types (3–5). The electrophysiological properties of Kv4 subtypes expressed in heterologous cells are, however, substantially different from those in native cells. Functional properties of some types of voltage-dependent K^+ channels are modified by the association of β subunits with α subunits (6–10). Although low-molecular-weight mRNA species and γ subunit of jellyfish *Shal* K^+ channel that modulate electrophysiological properties of α subunit of Kv4 subfamily were reported (11, 12), β subunit-like molecules of Kv4 subfamily have not been identified in mammalians. Very recently, three types of human K^+ channel-interacting proteins, KChIPs (hKChIP1-3), which specifically associate with the cytoplasmic N-termini of Kv4 subfamily, have been identified using the yeast two-hybrid systems (13). Electrophysiological experiments have also shown that the association of KChIPs with Kv4 subfamily elicits increment of current density, slower inactivation, and faster recovery from inactivation (13).

In the present study, we cloned cDNAs encoding novel splice variants of KChIP2 (KChIP2S/L) from rat, mouse, and human heart and also human umbilical vein endothelial cells (HUVECs) by RT-PCR cloning. It has been reported that a longer splice variant of Kv4.3 (Kv4.3L) is predominantly expressed in heart and smooth muscles of the rat (5). To examine that the cellular distribution of rat KChIP2S/L expressed in mammalian cells is greatly modified by the coexpression of Kv4.3L, immunoprecipitation of KChIP2 proteins with anti-Kv4.3 antibody and confocal imaging of GFP-fused KChIP2S/L and Kv4.3L labeled with fluorescent anti-Kv4.3 antibody were demonstrated.

MATERIALS AND METHODS

RNA extraction and reverse transcription. Total RNA extraction from the tissues of 9- to 10-week-old male Wistar rats and 3- to 4-week-old male *DDY* mice was performed by AGPC method (14). Human umbilical vein endothelial cells (HUVECs) were isolated and cultured as previously described by Muraki *et al.* (1997) (15). Cultured HUVECs were harvested by scraping using rubber policeman, and total RNA was extracted as described above. Total RNA ex-

[1] To whom correspondence should be addressed. Fax: +81-52-836-3431. E-mail: yimaizum@phar.nagoya-cu.ac.jp.

0006-291X/01 $35.00

tracted from human normal heart was purchased from BIOCHAIN. Using the extracted total RNA, reverse transcription (RT) was performed according to Gibco BRL's suggested protocol. Two microgram of total RNA and 200 ng of random hexamer (Roche Diagnostics) were heated for 10 min at 70°C and incubated for 10 min at 25°C for annealing. Each sample was incubated for 60 min at 42°C using 150 units of SUPERSCRIPT II RNase H^- reverse transcriptase (Gibco BRL) in solution containing 50 mM Tris–HCl (pH 8.3), 40 mM KCl, 6 mM $MgCl_2$, 1 mM DTT, and 1 mM individual dNTPs.

Polymerase chain reaction (PCR). The resulting cDNAs were subjected to PCR analysis in GeneAmp 2400 (Perkin–Elmer ABI) with AmpliTaq-Gold DNA polymerase (Perkin–Elmer ABI) using degenerated primers for human KChIP1-3 (GenBank Accession No. AF199597-9, respectively) and rat glyceralhyde-3-phosphate-dehydrogenase (X02231) as shown in Table 1. RT-PCR was performed under thermal cycle as follows: 5 s denaturation step at 94°C, 10 s annealing step at 55°C, 30 s extension step at 72°C. Amplified products were separated on 1.5% agarose gels in Tris acetate/EDTA buffer, visualized with 1 μg/ml ethidium bromide, and documented on FluorImager 595 (Molecular Dynamics). Next, they were cleaned using GENECLEAN II (BIO 101) and subcloned into plasmid vector, pBluescript II SK(+) (Stratagene) using TaKaRa ligation kit Ver. 1 (TaKaRa). Nucleotide sequences were determined by the dideoxynucleotide chain-termination method using Thermo Sequenase Cycle Sequencing kit (Amersham Pharmacia), with a DSQ-1000L sequencer (Shimadzu). The nucleotide sequences for degenerate primers were determined using 5′- and 3′- rapid amplification of cDNA ends (RACE) techniques.

Immunoprecipitation. To examine the interaction of KChIP2 with Kv4.3L in intact cells, COS-1 cells were transiently transfected with rat KChIP2S or KChIP2L expression plasmids together with a rat Kv4.3L expression plasmid or an original pcDNA3.1 (+) (Invitrogen) using LipofectAMINE (Gibco BRL) as previously described (16). Cells were grown for 48 h and then analyzed by immunoprecipitation followed by immunoblotting as described (17). Briefly, cells were lysed in 1.4 ml of lysis buffer (50 mM Tris–HCl, pH 7.5, 150 mM NaCl, 1% Triton X-100) containing a protease inhibitor cocktail (Roche Diagnostics). After incubation with unbound protein G agarose (Gibco BRL) for 2 h, cell lysates were centrifuged at 21,600*g* for 10 min at 4°C and the resulting supernatants were incubated with rabbit anti-rat Kv4.3 (Alomone Labs) (or anti-CALP2) (CALP: calsenilin-like protein) antisera and protein G agarose at 4°C overnight. Immunoprecipitates were washed twice in lysis buffer and analyzed by immunoblotting with anti-CALP2 (or anti-Kv4.3). Rabbit polyclonal antibody anti-CALP2 was originally raised against CALP, a KChIP3-like protein, fused to glutathione *S*-transferase, that also reacted with KChIP2S or KChIP2L (Morohashi Y *et al.* manuscript in preparation, and see lanes of "lysate" in Fig. 4).

GFP fluorescence images. Green fluorescence protein (GFP) was fused to the N-terminal of rat KChIP2S/L using NT-GFP Fusion TOPO Cloning Kit (Invitrogen). The resulting constructs, which we refer to pGFP-KChIP2S/L, were confirmed by DNA sequencing. As a control for the cellular distribution of unfused GFP, the original pcDNA3.1/NT-GFP (Invitrogen) was used. Kv4.3L-expressed and native HEK293 cells, which we refer to HEK-4.3L and HEK-N, respectively, were prepared and maintained as previously reported (5) and were transiently transfected using LipofectAMINE reagent. Cells were cultivated for 48–72 h after transfection and confocal images were viewed on a laser scanning confocal microscope (LSM510, Zeiss).

Immunocytochemistry. After observation of GFP fluorescence signals, HEK-N and HEK-4.3L were fixed with 3% paraformaldehyde for 10 min. They were subsequently permeabilized with PBS containing 0.2% Triton X-100. Non-specific binding sites were blocked with PBS containing 0.2% Triton X-100 and 1% normal goat serum (Solution A). Cells were then exposed to anti-Kv4.3 polyclonal antibody, diluted 1:50 dilution in Solution A for 24 h at 4°C. After washing excess primary antibody with PBS, the cells were exposed to biotin-conjugated goat anti-rabbit IgG (H & L) antibody (1:200 dilution, Chemicon) for 1 h at room temperature. After washing excess secondary antibody with PBS, the cells were labeled with rhodamine (TRITC)-conjugated streptavidin (1:50 dilution, Chemicon) for 1 h at room temperature. Digital images were viewed on a scanning confocal microscope (LSM510, Zeiss).

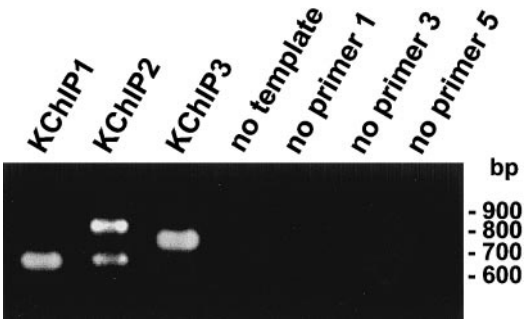

FIG. 1. Analysis of amplified products by 1.5% agarose gel electrophoresis. RT-PCRs were performed with three pair primers (primer 1, 3, 5, Table 1) for 40 cycles. cDNAs were obtained by reverse transcription of the total RNAs extracted from rat brain and heart, respectively. KChIP1: amplified products for primer 1. KChIP2: amplified products for primer 3. KChIP3: amplified products for primer 5. No template, no primer 1, no primer 3, and no primer 5: control reactions that lacked template cDNA, primer 1, primer 3, and primer 5, respectively. The migration of size-marker (100 bp DNA ladder) is shown on the right.

RESULTS AND DISCUSSION

Full length KChIP1-3 clones from rat brain (KChIP1 and 3) or heart (KChIP2) were PCR amplified with specific primers (primer 1 for KChIP1, primer 3 for KChIP2, and primer 5 for KChIP3) for 40 cycles. Amplified fragments were separated on 1.5% agarose gel electrophoresis. The PCR products for primer 1 and primer 5 were identified as dense bands by ethidium bromide staining at predicted sizes of 651 and 771 bp, respectively (Fig. 1, KChIP1 and KChIP3). Unexpectedly, for primer 3, double fragments of approximately 800 bp and 650 bp were identified, and the fragment of a predicted size (759 bp) was not detectable (Fig. 1, KChIP2). As a negative control to identify genomic DNA contamination, two other control reactions were used; one contained only primers and no template cDNA, and the other contained only template cDNA and no PCR primers. Control reactions that lacked template cDNA or PCR primer produced no band signal (Fig. 1, no template, no primer 1, 3, and 5).

KChIP1 cDNA derived from rat brain (rKChIP1) contains a 648 bp open reading frame that encodes a protein of 216 amino acids. The identity of nucleotide sequence of rKChIP1 with human KChIP1 (hKChIP1) was 94.8%. The amino acid sequence of rKChIP1 was nearly identical to hKChIP1, with the exception of one amino acid substitution at residue 72 (D in place of E, D72E). Similarly, KChIP3 cDNA derived from rat

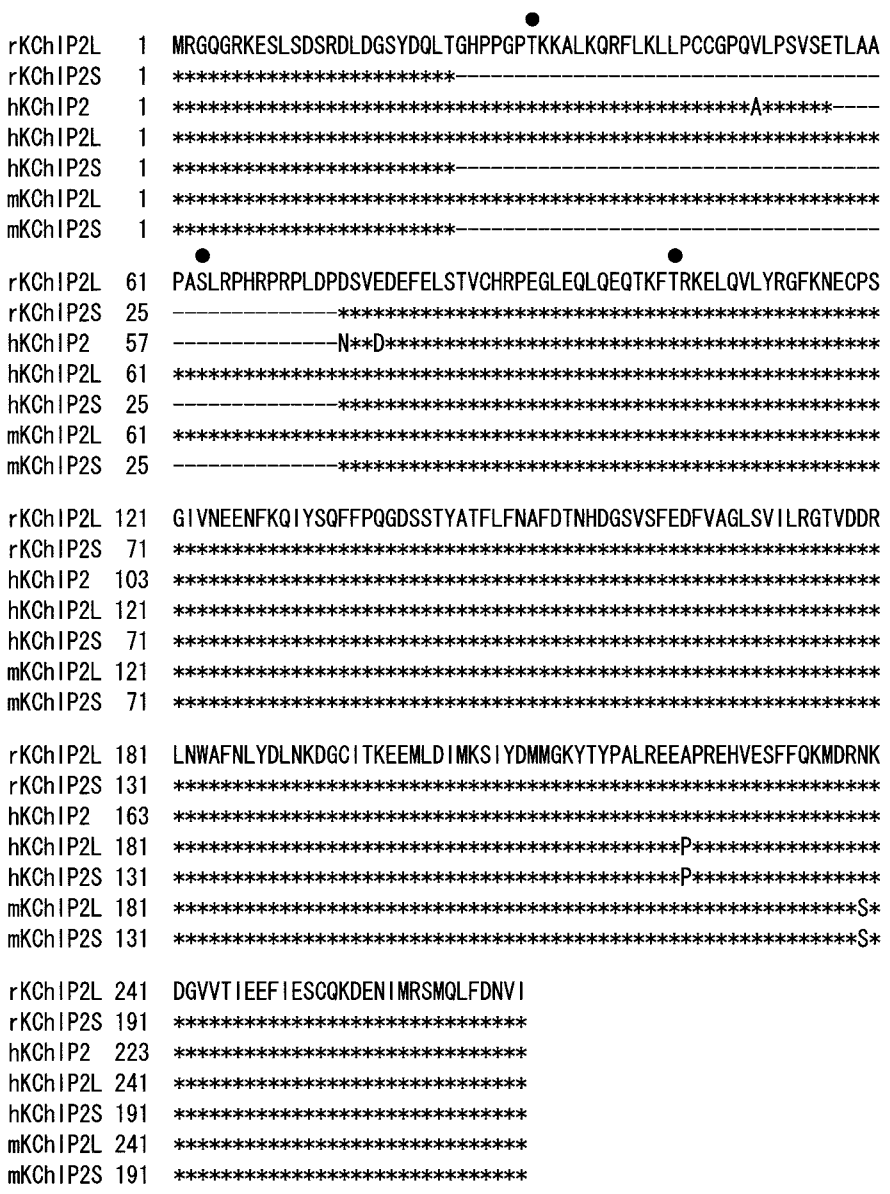

FIG. 2. Comparison of the amino acid sequences of the longer (KChIP2L) and shorter (KChIP2S) variants of KChIP2 of the rat (rKChIP2) with those of the human (hKChIP2) and mouse (mKChIP2). Residues that are identical to those of rKChIP2L were shown with asterisks. hKChIP2 sequence has been reported previously by An *et al.* [13]. Dashes indicate gaps introduced into sequence to improve alignment. (●) Consensus sequence for PKC phosphorylation.

brain (rKChIP3) contains a 768 bp open reading frame that encodes a protein of 256 amino acids. The extent of nucleotide sequence identity of rKChIP3 with human and mouse KChIP3 (hKChIP3 and mKChIP3) was 88.2 and 95.3%, respectively. The amino acid sequence identity of rKChIP3 with hKChIP3 and mKChIP3 was 93.8 and 98.4%, with 16 and 4 amino acid substitution, respectively (hKChIP3: T4A, A7V, M8T, P19L, R21H, I22T, R27K, F37L, T38S, I48V, A55T, S119A, L212A, Q220E, D233E, T228A; mKChIP3: M8V, G29S, Y181C, S247N). The same sequence data were obtained from at least five independent experiments.

DNA sequences of two amplified products for primer 3 described above were determined. They had high sequence similarities to but were substantially different from human KChIP2 (hKChIP2). We have termed these newly identified shorter and longer KChIP2 variants 'KChIP2S' and 'KChIP2L', respectively. KChIP2S and KChIP2L cDNAs derived from rat heart (rKChIP2S and rKChIP2L) contain 660 and 810 bp open reading frames that encode proteins of 220 and 270 amino acids, respectively (Fig. 2). In rKChIP2L, an insert region of 18 amino acids was found after residue 56, E (E56) of hKChIP2 reported by An *et al.* (13). In

TABLE 1

Oligonucleotide Sequences of Primers Used for RT-PCR

Primer number	Subtypes	Primer sequence: (+), sense; (−), antisense	Primer site	Product length (bp)
1	KChIP1 for RT-PCR cloning	(+) 5′-ATGGGGGCCGTCATGGGC-3′	1–18	651
		(−) 5′-TTACATGACATTTTGAAACAGCTGG-3′	651–627	
2	KChIP1	(+) 5′-CCGTCATGGGCACCTTCTCA-3′	8–27	356
		(−) 5′-TCCTCTCAGCAAAATCGACA-3′	363–344	
3	KChIP2 for RT-PCR cloning	(+) 5′-ATGCGGGGCCAGGGCCGC-3′	1–18	759
		(−) 5′-CTAGATGACATTGTCAAAGAGC-3′	759–738	
4	KChIP2	(+) 5′-GAGACCTGGACGGCTCCTAC-3′	41–60	
		(−) 5′-GACGGAGCCGTCGTGGTTGG-3′	330–311	290 (S)
			480–461	440 (L)
5	KChIP3 for RT-PCR cloning	(+) 5′-ATGCAGCCGGCTAAGGAAGT-3′	1–20	771
		(−) 5′-CTAGATGACATTCTCAAACA-3′	771–752	
6	KChIP3	(+) 5′-CAGACAGCAGTGACAGTGAA-3′	179–198	439
		(−) 5′-AGGATAGGGTAGGTGTGGC-3′	617–598	
7	GAPDH	(+) 5′-GCCATCACTGCCACTCA-3′	532–548	151
		(−) 5′-CAGTGAGCTTCCCGTTC-3′	682–666	

rKChIP2S, the residues from G25 to E56 of hKChIP2 were deleted. In the region except splicing sequences, the extent of nucleotide sequence identity of rKChIP2 with hKChIP2 was 95.4% and the amino acid sequence identity was 98.9%, with four amino acid substitution. The same sequence data were obtained from six independent experiments.

Database searches yielded no significant homology for the splicing residues of rKChIP2 with the other sequences submitted in GenBank database at either the nucleotide or amino acid levels. More than half of the splicing residues were composed of more than half of non-charged amino acids. Hydropathy analysis indicated no potential membrane spanning domains in rKChIP2L. rKChIP2L had two additional potential sites for phosphorylation by protein kinase C in the splicing residues (Fig. 2).

In addition, human KChIP2S and KChIP2L homologues (hKChIP2S/L), which are nearly identical to rKChIP2S and rKChIP2L, respectively, were isolated from human heart and umbilical vein endothelial cells (HUVECs). Surprisingly, as the results from several trials of RT-PCR experiments for 40 cycles, hKChIP2 clones reported previously by An *et al.* (13) were not detected in human heart and HUVECs. The two splice variants of KChIP2 were also identified in mouse heart (mKChIP2S/L). The splicing sequences of hKChIP2 and mKChIP2 were completely identical to those of rKChIP2, and the amino acid sequences of hKChIP2 and mKChIP2 were nearly identical to rKChIP2, with the exception of one amino acid substitution at residue 224/204 (A174/224P) (hKChIP2S/L) and 189/239 (N189/239S) (mKChIP2S/L), respectively (Fig. 2). The same sequence data were obtained from three (HUVECs) and six (human and mouse heart) independent experiments.

Based on these results, it is clear that the amino acid sequences of hKChIP2 reported by An *et al.* (13) were almost identical to those of KChIP2L in three species at residues 79–270. An *et al.* (13) have shown that the effects of hKChIP2Δ2-67 on Kv4.2 channel current properties are almost identical to those of the full-length hKChIP2, indicating that the N-terminus of hKChIP2 could not contribute to the modulation of Kv4 channel properties (13). The possibility that N-terminal splicing residues of KChIP2L may change the modulation of the Kv4 channel by KChIP2, however, remained to be determined.

Subsequently, the tissue-expression of KChIP1-3 was determined using RT-PCR (in rat: brain, heart, aorta, kidney, liver, lung, and pancreas; in mouse: brain, heart, aorta, and kidney; in human: heart and HUVECs). When RT-PCR at different cycle numbers (24−40 cycles at every 2 cycles) was performed using primer 2, 4, 6, and 7 as shown in Table 1, a linear relationship between the cycle number and the band density of PCR products was observed in the range of 26 to 36 cycles (not shown). Then, RT-PCR experiments were performed for 30 cycles and the specificity of each amplified product was confirmed by DNA sequencing.

Figure 3A showed that the expression patterns of KChIP transcripts in rat tissues. rKChIP1 and 3 transcripts were predominantly expressed in brain, whereas rKChIP2 in heart. These were consistent with the results from Northern blot analysis by An *et al.* (13), while the originally reported hKChIP2 was not observed in heart as shown above. In stead, rKChIP2S transcript but not rKChIP2L was highly expressed in heart. rKChIP1 transcripts were expressed at high levels also in kidney, at intermediate levels in aorta and lung, and at very weak or not detectable in liver and pancreas (Fig. 3A, KChIP1). On the other hand,

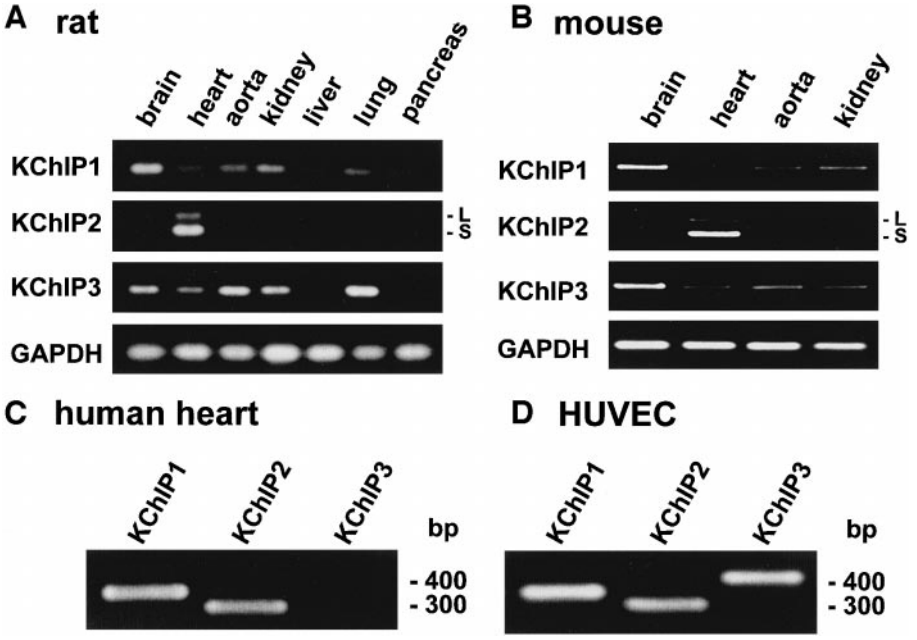

FIG. 3. Diverse expression of KChIP transcripts in rat (A) and mouse (B) tissues, human heart (C), and HUVECs (D). cDNAs were obtained by reverse transcription of the total RNAs and RT products were amplified by PCR using four pair-primers for KChIP1, KChIP2, KChIP3, and GAPDH (primer 2, 4, 6, 7, Table 1), under thermal cycle conditions of 94°C for 5 s, 55°C for 10 s and 72°C for 30 s, for 30 cycles. Amplified products were separated on 1.5% agarose gels. 356 bp (KChIP1), 440 bp (KChIP2L), 290 bp (KChIP2S), 439 bp (KChIP3), and 151 bp (GAPDH) fragments were identified by ethidium bromide staining, respectively. In C and D, the migration of size-marker (100 bp DNA ladder) is shown on the right.

rKChIP3 transcripts were expressed at high levels in aorta, kidney, and lung and at low levels or no detectable in liver and pancreas (Fig. 3A, KChIP3). In a 30 cycle PCR, rKChIP2 signals were observed in heart alone (Fig. 3A, KChIP2), but they were also observed in other tissues when PCR cycles were increased to 35 cycles (not shown). In contrast to the expression pattern of rKChIP2 in heart, expression levels of rKCHIP2L appears to be higher than those of rKChIP2S in brain, aorta, kidney, liver, lung, and pancreas. Similar expression levels of KChIP transcripts were observed in mouse tissues (brain, heart, aorta, and kidney) (Fig. 3B). GAPDH transcript was used to provide a basis for the comparison of KChIP transcripts (Fig. 3A and B, GAPDH). Of important, in human heart and HUVECs, hKChIP2S (290 bp) transcripts were expressed at high levels, whereas hKChIP2L (440 bp) and original hKChIP2 ones at very weak or no detectable levels by 30 cycle PCR (Fig. 3C and D).

To confirm that newly isolated rKChIP2S/L proteins associate with Kv4.3L channel proteins, intracellular interaction between rKChIP2 and Kv4.3 were examined by coimmunoprecipitation. When lysates of COS-1 cells transiently co-transfected with cDNAs encoding rKChIP2S or 2L and Kv4.3L were immunoprecipitated with anti-rat Kv4.3 antibody and then probed by immunoblotting with anti-CALP2, the immunoprecipitates were found to contain rKChIP2L or rKChIP2S, migrating at 27 or 35 kDa, respectively (Fig. 4A). Conversely, when lysates were immunoprecipitated with anti-CALP2 and then probed with anti-rat Kv4.3, a ~65 kDa polypeptide corresponding to Kv4.3L was specifically detected (Fig. 4B). These results were consistent with those from the yeast two-hybrid systems reported by An *et al.* (13), suggesting that rKChIP2S/L and Kv4.3L are able to form a complex in mammalian cells.

In addition, the subcellular localization of GFP-fused rKChIP2S/L in native and Kv4.3L-expressed HEK293 cells (HEK-N and HEK-4.3L) were visualized by laser scanning confocal microscopy. Fluorescence signals of plasma membrane were observed in GFP-fused rKChIP2S/L transfected HEK-4.3L (Fig. 5g and 5h) but not in GFP-fused rKChIP2S/L transfected HEK-N (Figs. 5b and 5c). As a control, unfused GFP fluorescence images were observed in HEK-N (Fig. 5a) and HEK-4.3L (Fig. 5f) transfected with GFP alone. Similar experiments were performed in Kv1.2- and Kv1.4-expressed HEK293 cells, resulting that diffuse fluorescence signals of GFP-fused rKChIP2S/L were observed in both cell lines (not shown).

After the measurement of GFP-fused rKChIP2S/L signals, cells were stained with the anti-Kv4.3 antibody by immunocytochemical procedures. The immunoreactivities to Kv4.3 were also visualized as the TRITC signals by confocal microscopy. The staining patterns of Kv4.3 were localized along plasma mem-

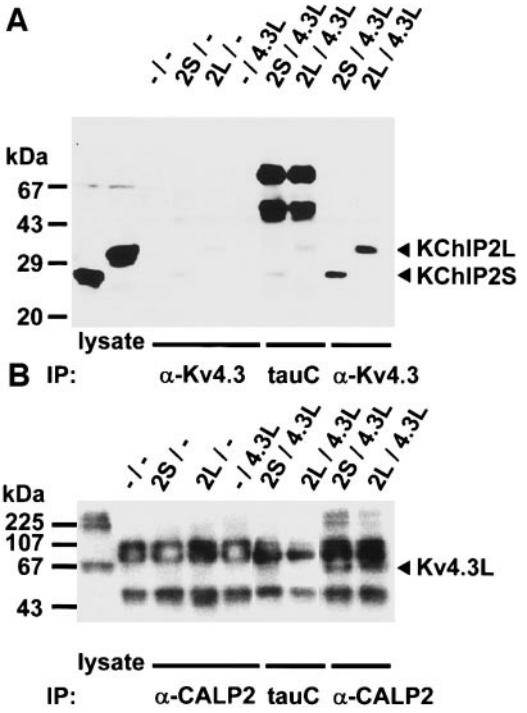

FIG. 4. Coimmunoprecipitation of KChIP2 with Kv4.3L. (A) Cell lysates of COS-1 cells transfected with cDNAs encoding KChIP2L or 2S and/or Kv4.3L were immunoprecipitated with an anti-Kv4.3 antibody (α-Kv4.3) or an irrelevant rabbit antisera (tauC against human tau protein) and probed by immunoblotting with anti-CALP2, which also recognized KChIP2S/L. Cell lysates of COS-1 cells transfected with cDNAs encoding KChIP2L or 2S prior to immunoprecipitation were analyzed in the left two lanes (lysate). Arrowheads indicate the migrating positions of KChIP2S/L, respectively. (B) Cell lysates were immunoprecipitated with anti-CALP2 antibody (α-CALP2) or an irrelevant antibody tauC and probed by immunoblotting with anti-rat Kv4.3 as in A. Cell lysates of COS-1 cells transfected with cDNAs encoding Kv4.3L prior to immunoprecipitation were analyzed in the lane at the left side (lysate). Arrowhead indicates the migrating position of Kv4.3L. Names of the transfected cDNAs (2L, KChIP2L; 2S, KChIP2S; 4.3L, Kv4.3L) and antibodies used for immunoprecipitation are indicated at the top and bottom of the panels, respectively. Molecular mass standards are shown in kilodaltons at the left side of the panels.

brane in GFP-fused rKChIP2S/L transfected HEK-4.3L (Figs. 5i and 5j) and were nearly identical to GFP fluorescence patterns of GFP-fused rKChIP2S/L (Fig. 5g and 5h), respectively. Pre-incubation with excess levels of antigen elicited the disappearance of Kv4.3 signals (not shown). As a control, diffuse staining patterns were observed in GFP-fused rKChIP2S/L transfected HEK-N (Figs. 5d and 5e).

In the present study, we cloned two novel splice variants of KChIP2; KChIP2L and 2S from rat, mouse, and human heart and HUVECs (Fig. 2) and showed that KChIP2S was a predominant isoform (Fig. 3). It is surprising that in human heart and HUVECs, the original hKChIP2 was not found. Although the reason is not clear, the existence of two splice variants was confirmed in three species, indicating the reliability of the present analyses. The functional difference between KChIP2L and 2S is a hot subject but remains to be determined. In rat and mouse tissues examined, KChIP transcripts (KChIP1-3) were expressed in differential expression patterns (Fig. 3). These results suggest that the assembly of different combinations of KChIPs with Kv4 members may considerably increase the complexity and diversity of A-type Kv channels in native cells.

KChIPs have four EF-hand motifs (13). Using EF-hand mutant of KChIP1, An *et al.* (13) have shown that modulation of Kv4 current properties by KChIP1 is dependent on Ca^{2+} (13). A-type K^+ channels in native cells have been regulated by Ca^{2+} indirectly via Ca^{2+}-dependent enzymes such as Ca^{2+}-dependent protein kinase C (PKC) and Ca^{2+}-calmodulin-dependent protein kinase II (CaMKII) (18–21). Kv4 members are the leading candidates of K^+ channel gene encoding I_A in many types of cells. Interestingly, Kv4.1 and 4.3 have consensus sequences for CaMKII phosphorylation in N-terminus (at residue 53). These strongly suggest that the EF-hand motifs of KChIPs may act as the Ca^{2+} buffering molecules in N-terminus of Kv4 members and thereby regulate the phosphorylation activity of CaMKII and/or PKC in native cells.

In cardiac and smooth muscle myocytes, physiological and pathophysiological alternations (e.g., development, pregnancy, and heart failure) cause the up- or down-regulation of I_A density (22–24). Therefore, the changes in the expression levels of KChIPs, in addition to Kv4 members, may involve in part of the up- or down-regulation of I_A density and even kinetics in such situations.

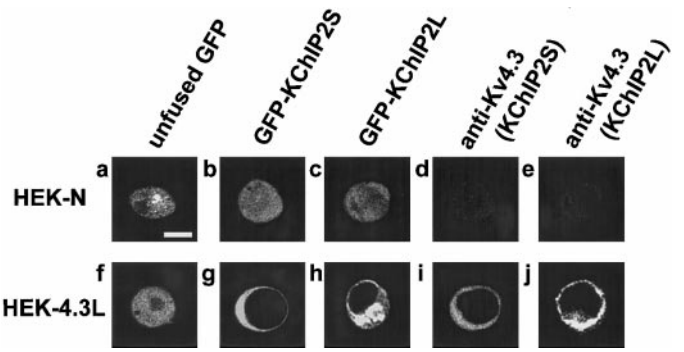

FIG. 5. Distribution of GFP-fused KChIP2S/L and Kv4.3 proteins in HEK-N and HEK-4.3L cells by confocal images. Fluorescence images of HEK-N (a–c) and HEK-4.3L (f–h) expressing unfused GFP (a, f), GFP-fused KChIP2S (b, g), or GFP-fused KChIP2L (c, h) are shown. After observation of GFP images, cells were stained with specific antibodies against Kv4.3 channel proteins using the avidin–biotin peroxidase technique. Antibody binding was detected with a rhodamine (TRITC)-conjugated streptavidin. d, e: HEK-N transfected with GFP-fused KChIP2S/L, respectively. i, j: HEK-4.3L transfected with GFP-fused KChIP2S/L, respectively. Images in b and d, c and e, g and i, and h and j were obtained from the same cells, respectively. The calibration bar represents 10 μm.

ACKNOWLEDGMENTS

This work was supported by Grant-in Aid for Scientific Research from the Japanese Ministry of Education, Science and Culture (to Y.I. and S.O.), by Grant-in Aid for Research in Nagoya City University (to S.O.), and by Research Grant for Cardiovascular Diseases (11C-1) from the Ministry of Health and Welfare (to Y.I.). We gratefully acknowledge support from Dr. I. Asamoto. The nucleotide sequence data reported have been submitted to the DDBJ, EMBL and GenBank nucleotide sequence databases with the Accession Nos. AB046443 (rat KChIP1), AB040032, (rat KChIP2L), AB040031 (rat KChIP2S), AB043892 (rat KChIP3), AB044584 (human KChIP2L), AB044585 (human KChIP2S), AB044570 (mouse KChIP2L), and AB044571 (mouse KChIP2S).

REFERENCES

1. Hille, B. (1992) Ionic Channels of Excitable Membranes, Sinauer Ltd, Sunderland, MA.
2. Nagano, N., Imaizumi, Y., and Watanabe, M. (1997) Effects of arachidonic acid on A-type potassium currents in smooth muscle cells of the guinea pig. *Am. J. Physiol. Cell Physiol.* **272,** C860–C869.
3. Serodio, P., Vega-Saenz de Miera, E., and Rudy, B. (1996) Cloning of a novel component of A-type K^+ channels operating at subthreshould potentials with unique expression in heart and brain. *J. Neurophysiol.* **75,** 2174–2179.
4. Fiset, C., Clark, R. B., Shimoni, Y., and Giles, W. R. (1997) Shal-type channels contribute to the Ca^{2+}-independent transient outward K^+ current in rat ventricle. *J. Physiol.* **500,** 51–64.
5. Ohya, S., Tanaka, M., Oku, T., Asai, Y., Watanabe, M., and Imaizumi, Y. (1997) Molecular cloning and tissue distribution of an alternatively spliced variant of an A-type K^+ channel α subunit, Kv4.3 in the rat. *FEBS Lett.* **420,** 47–53.
6. Rettig, J., Heinemann, S. H., Wunder, F., Lorra, C., Parcej, D. N., Dolly, J. O., and Pongs, O. (1994) Inactivation properties of voltage-gated K^+ channels altered by presence of β-subunit. *Nature* **369,** 289–294.
7. Tseng-Crank, J., Godinot, N., Johansen, T. E., Ahring, P. K., Strobaek, D., Mertz, R., Foster, C. D., Olesen, S. P., and Reinhart, P. H. (1996) Cloning, expression, and distribution of a Ca^{2+}-activated K^+ channel beta-subunit from human brain. *Proc. Natl. Acad. Sci. USA* **93,** 9200–9205.
8. Sanguinetti, M. C., Curran, M. E., Zou, A., Shen, J., Spector, P. S., Atkinson, D. L., and Keating, M. T. (1996) Coassembly of K_VLQT1 and minK (IsK) proteins to form cardiac I_{Ks} potassium channel. *Nature* **384,** 80–83.
9. Abbott, G. W., Sesti, F., Splawski, I., Buck, M. E., Lehmann, M. H., Timothy, K. W., Keating, M. T., and Goldstein, S. A. N. (1999) MiRP1 forms I_{Kr} potassium channels with HERG and is associated with cardiac arrhythmia. *Cell* **97,** 175–187.
10. Perez-Garcia, M. T., Lopez-Lopez, J. R., and Gonzalez, C. (1999) Kvβ1.2 subunit coexpression in HEK293 cells confer O2 sensitivity to Kv4.2 but not Shaker Channels. *J. Gen. Physiol.* **113,** 897–907.
11. Jegla, T., and Salkoff, L. (1997) A novel subunit for shal K^+ channels radically alters activation and inactivation. *J. Neurosci.* **17,** 32–44.
12. Chabala, L. D., Bakry, N., and Covarrubias, M. (1993) Low molecular weight poly(A)$^+$ mRNA species encode factors that modulate gating of a non-Shaker A-type K^+ channel. *J. Gen. Physiol.* **102,** 713–728.
13. An, W. F., Bowlby, M. R., Betty, M., Cao, J., Ling, H. P., Mendoza, G., Hinson, J. W., Mattsson, K. I., Strassle, B. W., Trimmer, J. S., and Rhodes, K. J. (2000) Modulation of A-type potassium channels by a family of calcium sensors. *Nature* **403,** 553–556.
14. Chirgwin, J. M., Przybyla, A. E., McDonald, R. J., and Rutter, W. J. (1979) Isolation of biologically active ribonucleic acid from sources enriched in ribonuclease. *Biochemistry* **18,** 5294–5299.
15. Muraki, K., Imaizumi, Y., Ohya, S., Sato, K., Takii, T., Onozaki, K., and Watanabe, M. (1997) Apamin-sensitive Ca^{2+}-dependent K^+ current and hyperpolarization in human endothelial cells. *Biochem. Biophys. Res. Commun.* **236,** 340–343.
16. Tomita, T., Maruyama, K., Saido, T. C., Kume, H., Shinozaki, K., Tokuhiro, S., Capell, A., Walter, J., Gruenberg, J., Haass, C., Iwatsubo, T., and Obata, K. (1997) The presenilin 2 mutation (N141I) linked to familial Alzheimer disease (Volga German families) increases the secretion of amyloid β protein ending at the 42nd (or 43rd) residue. *Proc. Natl. Acad. Sci. USA* **94,** 2025–2030.
17. Tomita, T., Takikawa, R., Koyama, A., Morohashi, Y., Takasugi, N., Saido, T. C., Maruyama, K., and Iwatsubo, T. (1999) C terminus of presenilin is required for overproduction of amyloidogenic Aβ42 through stabilization and endoproteolysis of presenilin. *J. Neurosci.* **19,** 10627–10634.
18. Hoffman, D. A., and Johnston, D. (1998) Downregulation of transient K^+ channels in dendrites of hippocampal CA1 pyramidal neurons by activation of PKA and PKC. *J. Neurosci.* **18,** 3521–3528.
19. Nakamura, T. Y., Coetzee, W. A., Vega-Saenz De Miera, E., Artman, M., and Rudy, B. (1997) Modulation of Kv4 channels, key components of rat ventricular transient outward K^+ current, by PKC. *Am. J. Physiol. Heart Circ. Physiol.* **273,** H1775–H1786.
20. Tessier, S., Karczewski, P., Krause, E. G., Pansard, Y., Acar, C., Lang-Lazdunski, M., Mercadier, J. J., and Hatem, S. N. (1999) Regulation of the transient outward K^+ current by Ca^{2+}/calmodulin-dependent protein kinases II in human atrial myocytes. *Circ. Res.* **85,** 810–819.
21. Koh, S. D., Perrino, B. A., Hatton, W. J., Kenyon, J. L., and Sanders, K. M. (1999) Novel regulation of the A-type K^+ current in murine proximal colon by calcium-calmodulin-dependent protein kinase II. *J. Physiol.* **517,** 75–84.
22. Kaab, S., Dixon, J., Duc, J., Ashen, D., Nabauer, M., Beuckelmann, D. J., Steinbeck, G., McKinnon, D., and Tomaselli, G. F. (1998) Molecular basis of transient outward potassium current downregulation in human heart failure: a decrease in Kv4.3 mRNA correlates with a reduction in current density. *Circulation* **98,** 1383–1393.
23. Wang, S. Y., Yoshino, M., Sui, J. L., Wakui, M., Kao, P. N., and Kao, C. Y. (1998) Potassium currents in freshly dissociated uterine myocytes from nonpregnant and late-pregnant rats, *J. Gen. Physiol.* **112,** 737–756.
24. Crumb, W. J., Jr., Pigott, J. D., and Clarkson, C. W. (1995) Comparison of Ito in young and adult human atrial myocytes: evidence for developmental changes. *Am. J. Physiol. Heart Circ. Physiol.* **268,** H1335–H1342.